Migration of Open Volume Deficiencies in Hydrogenated Amorphous Silicon during Annealing

Melskens, Jimmy; Eijt, Stephan W H; Schouten, Marc; Vullers, Albert S.; Mannheim, Awital; Schut, Henk; Macco, Bart; Zeman, Miro; Smets, Arno H M

DOI
10.1109/JPHOTOV.2016.2646421

Publication date
2017

Document Version
Accepted author manuscript

Published in
IEEE Journal of Photovoltaics

Citation (APA)
Melskens, J., Eijt, S. W. H., Schouten, M., Vullers, A. S., Mannheim, A., Schut, H., Macco, B., Zeman, M., & Smets, A. H. M. (2017). Migration of Open Volume Deficiencies in Hydrogenated Amorphous Silicon during Annealing. *IEEE Journal of Photovoltaics*, *7*(2), 421-429. Article 7828138. https://doi.org/10.1109/JPHOTOV.2016.2646421

The migration of open volume deficiencies in hydrogenated amorphous silicon during annealing

Jimmy Melskens[1,4(*)], Stephan W.H. Eijt[2], Marc Schouten[1], Albert S. Vullers[1], Awital Mannheim[2], Henk Schut[3], B. Macco[4], Miro Zeman[1], and Arno H.M. Smets[1]

[1] Photovoltaic Materials and Devices, Faculty of Electrical Engineering, Mathematics and Computer Science
[2] Fundamental Aspects of Materials and Energy, Faculty of Applied Sciences
[3] Neutron and Positron Methods in Materials, Faculty of Applied Sciences
[1,2,3] Delft University of Technology, The Netherlands
[4] Department of Applied Physics, Eindhoven University of Technology, The Netherlands
[*] Current affiliation

***Abstract* — The nanostructure of hydrogenated amorphous silicon (a-Si:H) is studied by means of Doppler broadening positron annihilation spectroscopy (DB-PAS) and Fourier transform infrared (FTIR) spectroscopy. The evolution of open volume deficiencies is monitored during annealing, demonstrating that small vacancies and other small vacancy clusters that are initially present in the a-Si:H structure agglomerate into larger vacancy clusters. The migration of open volume deficiencies is less pronounced for a-Si:H deposited at higher hydrogen-to-silane gas flow rate ratio, *R*. FTIR spectroscopy reveals the presence of a peculiar peak in the refractive index in the infrared – and hence the calculated mass density – which occurs just before H effusion from the films starts. The combined results of DB-PAS and FTIR spectroscopy indicate that a stress buildup caused by the accumulation of H_2 in agglomerating vacancies during annealing can explain the sudden mass density increase. At higher temperatures, stress is released with the onset of H effusion. The H effusion consists of a two-stage process involving small open volume deficiencies and nanosized voids, respectively, contrasting earlier interpretations. The reduced amount of hydrogen migration and enhanced hydrogen passivation degree are suggested as key factors to the reduced light-induced degradation associated with increased *R* values.**

***Index Terms* — Defects, hydrogenated amorphous silicon (a-Si:H), nanostructure, vacancies, annealing.**

I. Introduction

In the past five decades, hydrogenated amorphous silicon (a-Si:H) has found its way from the academic lab environment to a multitude of applications, such as sensors and thin film transistors [1], as well as various types of solar cells. Especially notable examples include multi-junction thin film silicon (TF Si) solar cells and silicon heterojunction (SHJ) solar cells [2], the latter of which have enabled the current world record conversion efficiency for silicon solar cells [3]. Despite the vast amount of fundamental research on a-Si:H that was needed to realize these achievements, there is still no clear understanding of the a-Si:H nanostructure and the defects therein due to the nanostructural complexity of a-Si:H materials. Often the nanostructure is described as a continuous random network (CRN) where isolated dangling bonds are the dominant defects [4]. In the CRN, threefold-coordinated Si atoms have direct control over midgap states [5],[6]. The paramagnetic nature of dangling bonds has been analyzed by means of electron paramagnetic resonance (EPR) [7]-[9]. Additionally, it has been suggested that dangling bonds can be converted into weak bonds and therefore also impact the tail states [10]-[13], which to a certain extent likely act as defects as well. Alternatively, floating bonds, *i.e.* fivefold-coordinated Si atoms, have also been suggested as possible defects, but this idea never attracted wide support since floating bonds have only appeared in modelling studies while experimental observations are lacking [14]-[17].

Although it is clear that hydrogen (H) plays an important role in reducing the defect density, the exact mechanism behind the hydrogen passivation of dangling bonds is unclear. The nature of the defects and the hydrogen passivation in the bulk of the material are particularly important matters when trying to understand the light-induced degradation (LID) of a-Si:H, also known as the Staebler-Wronski effect (SWE) [18],[19], which has been very intensively investigated in films and solar cells with one or more junctions based on a-Si:H [8],[14],[20]-[40]. The formation of defects in a-Si:H has been linked to strained bonds [41]-[44] and migrating hydrogen [45]-[47], but always with a CRN view on the nanostructure. However, several experimental results have questioned the correctness of the CRN in describing the nanostructure [48]-[51]. Furthermore, recent EPR studies have suggested that uniformly distributed isolated dangling bonds are not the only defects in a-Si:H and at least two types of defects are involved in the SWE [52]-[54]. An alternative to the CRN is the so-called disordered network with hydrogenated vacancies (DNHV) [55],[56], which has recently made it possible to correlate the a-Si:H nanostructure to the open-circuit voltage of a-Si:H solar cells [57]. In the DNHV, not only the migration of hydrogen in a-Si:H can be considered, but also the migration of open volume deficiencies, such as divacancies (DV), multivacancies (MV), and nanosized voids (NV), which are surrounded by disordered, CRN-like regions.

However, the hydrogen passivation degree of open volume deficiencies in the DNHV is still unknown due to a lack of characterization techniques that can directly probe this. Therefore, the objective of this study is to investigate the diffusion of both hydrogen and open volume deficiencies in a-Si:H while using annealing as a tool to study the nanostructure. In particular, we use the combination of Doppler broadening positron annihilation spectroscopy (DB-PAS) and Fourier transform infrared (FTIR) spectroscopy to monitor the evolution of and interplay between open volume deficiencies and hydrogen as a function of temperature.

In this work, we demonstrate a clear agglomeration of divacancies and other small vacancy clusters into larger open volume deficiencies in the temperature range up to 400 °C using DB-PAS. FTIR spectroscopy on the other hand indicates that, simultaneously, a significant amount of molecular hydrogen, which becomes mobile during the agglomeration of DVs into larger vacancy clusters, is trapped in open volume deficiencies. This leads to a pronounced local stress build up which is subsequently released upon effusion of trapped hydrogen, as revealed by a peculiar peak in the temperature dependence of the refractive index in the infrared part of the spectrum. Finally, this study reveals that at higher temperatures, a second stage of hydrogen effusion occurs, now involving the release of hydrogen liberated from Si-H bonds at the surfaces of the larger open volume deficiencies such as NVs.

II. Experiment

A. Sample definitions

In this work, we study a series of five 412 ± 16 nm thick a-Si:H films deposited by plasma-enhanced chemical vapor deposition (PECVD) on Corning XG glass and crystalline silicon substrates. Note that these relatively thick films were analyzed instead of the more standard a-Si:H layer thicknesses of ~70-350 nm that are typically used in state-of-the-art TF Si single-junction [32,36,37], tandem [33,37,58], triple-junction [31,38], and quadruple-junction [35,39,59] solar cells. In this way, a clear plateau appears on the positron depth profile in the DB-PAS measurements which enables a more accurate determination of the Doppler *S*-*W* values of the film. This determination is further enhanced by performing the DB-PAS measurements on the a-Si:H films on glass substrates only, since the contrast in *S*-*W* values is significantly larger between a-Si:H and glass in comparison to a-Si:H and c-Si. The H_2-SiH_4 gas flow rate ratio, $R = [H_2] / [SiH_4]$, was varied from $R = 0$ to $R = 10$, since it is known that the light soaking stability can be improved when increasing R [29],[60]-[63], while the responsible nanostructural reason is unclear. Note that the pressure was set at $p = 0.7$ mbar for the $R = 0$ films and $p = 2$ mbar for the $R = 2.5$-10 films, as it was not possible to ignite and sustain a stable plasma at lower pressures for the $R > 0$ conditions. For all depositions a substrate temperature of $T_s = 180$ °C was set and the rf power was fixed at $P_{rf} = 0.022$ W/cm^2. Due to the decreasing silane partial pressure when increasing R, the deposition rate decreased from $r_d = 11.1$ nm/min ($R = 0$) to $r_d = 6.6 \pm 0.7$ nm/min ($R = 2.5$-10) [64]. It is noted that the samples do not lie on the same point of the Paschen curve as illustrated by the obvious differences in p and r_d, while this is known to be a way to distinguish different types of a-Si:H and their light soaking stability [32]. However, the particular samples discussed in this work can still be compared, since the deposition conditions with the lowest and highest R values are known from previous work to yield solar cells with a significantly different light soaking stability [29,65]. The samples with R values in between 0 and 10 have been added to display possible trends with more statistical certainty.

All films were co-deposited on both substrate types to mitigate the nanostructural differences between each pair of films. Such subtle differences might occur due to differences in thermal conductivity for glass and c-Si, which can in turn result in small differences in surface roughness of the a-Si:H films grown on the two substrate types. Another possible reason is the generally surface roughness dependent growth of Si:H and the amorphous-to-crystalline transition that typically occurs when growing in $R > 0$ conditions up to a sufficiently large thickness [32],[66]-[68]. However, possible differences in surface roughness are likely to be very small, since all substrates are atomically flat and any effects of the surface are likely to be negligible when analyzing the bulk properties of relatively thick films, which is the focus of this work. Since Raman measurements (executed with a Renishaw system equipped with a 514 nm laser) show no significant differences between the various samples and confirm that all films investigated here are fully amorphous, we conclude that a combined analysis of the DB-PAS measurements on the films on glass together with the FTIR measurements on the films on c-Si substrates is justified.

B. Analysis of the nanostructure: characterization approach

DB-PAS is employed to detect the dominant type of open volume deficiency in the material, while FTIR spectroscopy enables an investigation of the environment of Si-H bonds [50]. The positron Doppler broadening of the 511 keV annihilation radiation was measured using positrons with a tunable kinetic energy in the range of 0-25 keV. The Doppler S and W parameters were determined using momentum windows for S and W of $|p| < 3.0 \cdot 10^{-3}$ m_0c and $8.2 \cdot 10^{-3}$ $m_0c < |p| < 23.4 \cdot 10^{-3}$ m_0c, respectively, with m_0 and c representing the electron rest mass and the speed of light in vacuum. The S parameter is a measure for positron annihilation with valence electrons, which provides sensitivity to the electronic structure and the presence of open volume deficiencies such as vacancies or vacancy clusters. The increase in size of vacancies or vacancy clusters in an otherwise identical material generally leads to an increase in the S parameter. The W parameter is a measure of annihilation with (semi)core electrons which provides chemical sensitivity to the positron trapping site. Generally, dense material is characterized by a relatively low S value and a relatively high W value, while opposite values of S and W typically indicate porous material. The S and W depth profiles were analyzed using the VEPFIT program [69]. The detailed procedure for the positron Doppler broadening depth profiling method is described in Ref. [70]. A variable energy positron beam with an intensity of 10^5 e^+/s and a diameter of 8 mm at the position of the sample is obtained via moderation of positrons which are emitted through a tungsten foil from a ^{22}Na source to

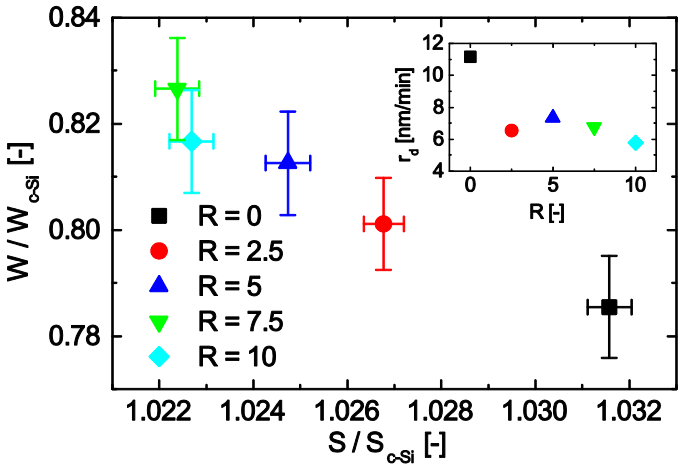

Fig. 1. Evolution of $S/S_{c\text{-}Si}$ and $W/W_{c\text{-}Si}$ for a series of a-Si:H films where the silane-to hydrogen gas flow rate ratio, R, was varied. The more dense type of a-Si:H is characterized by lower values of $S/S_{c\text{-}Si}$. Note that the error bars are given by the VEPFIT program [69,70] as fitting errors. The deposition rates for the different values of R are indicated in the inset.

execute the DB-PAS measurements. The interested reader is referred to Refs. [71] and [72] for more details on the DB-PAS experimental setup used in this work and Ref. [73] for further information about the DB-PAS technique in general.

FTIR measurements were conducted on the a-Si:H films deposited on c-Si substrates using a Thermo Fisher Nicolet 5700 FTIR spectrometer in transmission mode to obtain the intensities of the Si-H low and high stretching modes (LSM; HSM) and wagging modes (WM). The LSM ($\omega \approx 2000$ cm^{-1}) are indicative of Si-H bonds in DVs while the HSM ($\omega \approx 2100$ cm^{-1}) are characteristic for large vacancy clusters such as NVs [49,50,55-57]. The summed intensities of the WM ($\omega \approx 610$ cm^{-1} and $\omega \approx 650$ cm^{-1}) are used to calculate the mass density of the film, $\rho_{a\text{-}Si:H,WM}$, and the atomic hydrogen content, $c_{H,WM}$.

III. Results and Discussion

A. Detection of open volume deficiencies in as-deposited a-Si:H

First, all the samples were characterized by DB-PAS to establish how R affects the dominant open volume deficiency in the as-deposited state. The measured positron implantation depth profiles were fitted using the VEPFIT program to finally obtain the Doppler S and W parameters of the films [69],[70]. We report normalized $S/S_{c\text{-}Si}$ and $W/W_{c\text{-}Si}$ values to enable a comparison with literature values. A reference c-Si sample was measured for this purpose. The VEPFIT results on as-deposited films are shown in Fig. 1 to indicate the variation in open volume deficiencies upon varying the deposition parameter R. Strikingly, increasing R leads to a decrease in $S/S_{c\text{-}Si}$ while it is commonly known that increasing R can yield a reduced LID [29],[60]-[63]. This implies that the extra hydrogen in the plasma when increasing R decreases the open volume that is available for the positron to reside in. It is noted that the $R = 10$ material exhibits a slightly higher $S/S_{c\text{-}Si}$ value and a slightly lower $W/W_{c\text{-}Si}$ value with respect to the $R = 7.5$ sample, but this variation in S-W values still falls within the error bars shown in Fig. 1, as given by the VEPFIT program. The similarity in S-W values for $R = 7.5$ and $R = 10$ can be understood as a saturation of the open volume reduction that is induced by the extra hydrogen in the plasma, in analogy to the saturation in LID reduction that typically sets in for sufficiently large R values. Until this saturation is reached, the size of the dominant open volume deficiency in the deposited film is thus decreased and/or the hydrogen passivation degree of open volume deficiencies is enhanced. If the latter is the case, this would imply that H_2 dilution results in more stable a-Si:H because of an improved hydrogen passivation degree of dangling bonds present at the surfaces of open volume deficiencies. This hypothesis is supported by recent EPR results which suggest that defects on the surfaces of vacancy clusters play a role in the SWE [53],[54]. Note that a SWE model that mentions the relevance of open volume deficiencies and hydrogen motion on the surface of NVs was already introduced by Carlson three decades ago but never gained wide acceptance [74],[75]. Interestingly, in that model, fewer dimer reconstructions occur when the hydrogen passivation degree of vacancies is enhanced, which is in line with our findings.

B. Stability of open volume deficiencies in a-Si:H during annealing

More insight into the stability of open volume deficiencies that are dominant in a-Si:H films deposited at different R values can be gained by monitoring $S/S_{c\text{-}Si}$ and $W/W_{c\text{-}Si}$ during *in situ* annealing experiments. It is particularly interesting to investigate how R affects the migration of open volume deficiencies during annealing, since the annealing behavior was previously only investigated for $R = 0$ material [50]. All films were isochronally annealed for 1 h at temperatures increasing from 50 °C to 800 °C in steps of 50 °C at 10^{-7} mbar. The samples were cooled down to room temperature in the vacuum to minimize effects of oxidation on the measurements and all measurements were conducted at room temperature. Note that the DB-PAS samples stayed in the measurement system for the entire duration of the annealing experiment to exclude any oxidation effects on the measurements altogether. The FTIR samples were annealed using the deposition chamber and fully cooled down in the load-lock before the short but necessary vacuum break to transport the samples to the FTIR setup. Although this means that oxidation of the films could take place, this effect is unlikely to significantly affect the measurement data since the films were never exposed to air for more than one minute and the ultrathin oxide that could possibly form would in any case be orders of magnitude smaller than the film thickness. After each annealing step, DB-PAS and FTIR spectroscopy were employed to monitor nanostructural changes in the films.

Best fits for the positron depth profiles were obtained with a model consisting of two layers that make up the a-Si:H film, *i.e.* a top layer and a bottom layer, due to the annealing-induced changes. The top and bottom layer show small quantitative differences but otherwise similar trends in S and W upon annealing. The VEPFIT results corresponding to the annealing experiments conducted on the $R = 0$, $R = 5$, and $R = 10$ films are shown in Fig. 2. Only the results for the top layer are shown

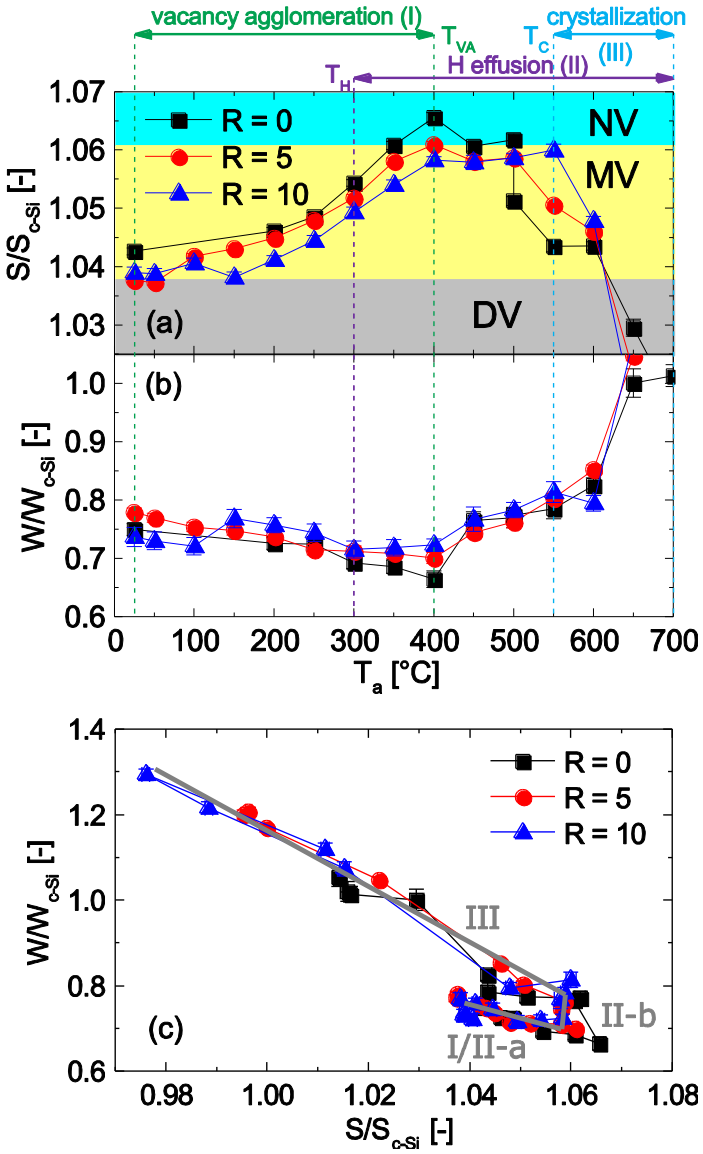

Fig. 2. VEPFIT results for three dense a-Si:H films deposited at different R values annealed *in situ* at subsequently increased annealing temperatures showing the evolution of the (a) $S/S_{c\text{-}Si}$ and (b) $W/W_{c\text{-}Si}$ parameters of the top layer of the films. The same data are used to form an (c) S-W plot for the top layers of these three a-Si:H films; the grey lines are added as a guide to the eye. Note that the error bars are given by the VEPFIT program [69,70] as fitting errors. Note that the annealing treatment at T_a = 500 °C was conducted twice with a break of 3 months in between due to technical reasons.

because the implanted positron is more sensitive to changes in the top layer although the bottom layer results are similar. Note that the positron is generally more sensitive to changes in the top layer, owing to the better depth resolution at low positron implantation energies. Based on DB-PAS and FTIR spectroscopy, three different processes can be identified during annealing: vacancy agglomeration, H effusion, and crystallization [50]. These processes are labelled as I, II, and III, respectively. Process I is characterized by an increase in $S/S_{c\text{-}Si}$, starting at values characteristic for the presence of DVs but steadily increasing into the MV and NV ranges. Note that agglomeration of large vacancy clusters during annealing around 300-400 °C has also been reported based on small angle X-ray scattering (SAXS) [76] and nuclear magnetic resonance (NMR) [77],[78]. In our study, FTIR spectroscopy shows that hydrogen effusion starts at around 300 °C (process II) [50], as will become clear from the FTIR data shown in Fig. 3a. The $S/S_{c\text{-}Si}$ values first increase while the $W/W_{c\text{-}Si}$ values decrease up to a temperature of ~400 °C. Beyond 550 °C, the $S/S_{c\text{-}Si}$ values show a significant decrease (and the $W/W_{c\text{-}Si}$ values a significant increase) for all samples, characteristic for crystallization of the films (process III). Note that Raman measurements pointed out that at the end of the annealing experiments (at T_a = 800 °C) all films had indeed completely crystallized and showed no signature of any Si-H bonds in the material. While processes I, II, and III appear for all samples, there are small yet qualitative differences in the evolution of $S/S_{c\text{-}Si}$ and $W/W_{c\text{-}Si}$ for the three films. For an annealing temperature, T_a, of 400 °C and less, it can be concluded that a higher T_a is needed to achieve the same $S/S_{c\text{-}Si}$ value with increasing R. This implies that vacancy agglomeration evolves less efficiently in high R materials, *i.e.* additional energy is needed to arrive at similarly sized open volume deficiencies by annealing in the more stable, high R materials in comparison to the low R materials. Alternatively, one might infer that in the same T_a range $S/S_{c\text{-}Si}$ is always higher for the lower R materials and the increase in $S/S_{c\text{-}Si}$ is similar for all R materials, so although vacancy clustering is clearly taking place, this would mean that there are no significant differences in this vacancy clustering process between the different R materials. However, based on the generally larger qualitative differences between the three datasets for 400 < T_a < 600 °C, and in particular the differences at T_a = 550 °C, we suggest that different annealing behavior can indeed be recognized here and both the migration of open volume deficiencies and the hydrogen effusion during annealing are likely to evolve with greater difficulty in the higher R material. More simply put, vacancies in more stable, higher R materials appear to migrate less easily during annealing. We thus suggest that the material which exhibits the most limited amount of open volume deficiency migration has the smallest LID.

Now that processes I, II, and III have been identified, the question is what the detailed differences in these processes are upon variation of R. Therefore, the annealing data from Fig. 2a and 2b are visualized in an S-W plot, as depicted in Fig. 2c, so the different states of the films and the transitions between them become more obvious. The S-W points of the different states of the film are connected by three edges which each represent a different process that takes place in the film during annealing. For example, based on the $S/S_{c\text{-}Si}$ increase in Fig. 2a, it can be concluded that vacancy agglomeration is dominant when $T_a \leq$ 400 °C, leading to a shift in the S-W point from its initial position for as-deposited films towards the bottom-right part of Fig. 2c for all three samples. Although three edges can be recognized here, they do not exactly correspond to the three processes I, II and III identified in Figs. 2a and 2b. Namely, as demonstrated by the FTIR data discussed below, a certain fraction of Si-H bonds is already breaking when $T_a \leq$ 400 °C, starting from temperatures of ~300 °C. The hydrogen effusion associated with this breaking of Si-H bonds could come from small open volume deficiencies like DVs which agglomerate into larger vacancies. Furthermore, there is no increase in

$W/W_{c\text{-}Si}$ for $T_a \leq 400$ °C which would indicate a lower hydrogen content with respect to the hydrogen content in the as-deposited state. This type of hydrogen effusion is labelled as process II-a in Fig. 2c. Only when $T_a > 400$ °C, $W/W_{c\text{-}Si}$ clearly increases while $S/S_{c\text{-}Si}$ is fairly constant (R = 5, 10) or decreases (R = 0), indicating that hydrogen effusion becomes dominant over vacancy agglomeration. This latter type of hydrogen effusion could arise from Si-H bond breaking in large open volume deficiencies like NVs, depleting the surfaces of hydrogen. During this process, increasingly more Si core states are probed by positrons trapped in the open volume deficiencies, visible in the strong increase in $W/W_{c\text{-}Si}$, and this process is labelled as II-b in Fig. 2c. Finally, a strong decrease in $S/S_{c\text{-}Si}$ and a large increase in $W/W_{c\text{-}Si}$ is seen for the crystallization process III, moving the S-W point of the increasingly dense layer towards the top-left part of the S-W diagram.

C. Changes in Si-H bonds during annealing

Since the structural material changes have now been revealed by DB-PAS, it is interesting to investigate the changes in Si-H bonds through FTIR spectroscopy. This is particularly important in order to understand how the hydrogen effusion takes place in the nanostructure. The suggested different types of hydrogen effusion during annealing are clearly revealed when considering the evolution of the integrated absorption strength of the Si-H wagging modes, which is used to calculate the mass density of the film, $\rho_{a\text{-}Si:H,WM}$, and the atomic hydrogen content, $c_{H,WM}$, using previously defined proportionality constants and the Clausius-Mosotti equation [50],[55],[79]. Another input parameter for this equation is the refractive index in the infrared part of the spectrum, n_∞, which is determined from fitting the background contribution in the FTIR measurement, *i.e.* those parts of the spectrum which do not contribute to either the WM or stretching modes (SM) [80]. The evolution of $\rho_{a\text{-}Si:H,W}$, $c_{H,WM}$, and n_∞ during annealing are shown in Fig. 3.

When considering $c_{H,WM}$ it is obvious that the hydrogen effusion due to breaking Si-H bonds starts when $T_a > 300$ °C and the $c_{H,WM}$ decrease is independent of R. Also $\rho_{a\text{-}Si:H,WM}$ is independent of R in the as-deposited state and the calculated values (2.23-2.24 g/cm^3) indicate that all films are dense [55]. During annealing a gradual densification is observed, mostly due to hydrogen effusion, but interestingly $\rho_{a\text{-}Si:H,WM}$ increases to a very high value in a narrow temperature interval around T_a = 300 °C, and reaches values which are even beyond the c-Si density. As is shown in Fig. 3c, it is clear that this surprising result is due to a sharp increase of the refractive index, n_∞, which lowers again when $T_a > 300$ °C. Based on the minimal differences in the data trends shown in Figs. 3b and 3c, it is noted that $\rho_{a\text{-}Si:H}$ is much more strongly determined by n_∞ than it is by c_H, so the sudden increase in the calculated $\rho_{a\text{-}Si:H}$ value is clearly due to a sharp increase in n_∞ [55],[79]. A simple, highly likely mechanism for this temporary increase in $\rho_{a\text{-}Si:H,WM}$ is the accumulation of H_2 in open volume deficiencies during vacancy agglomeration. For example, when two fully H-passivated DVs cluster together into a tetravacancy, a H_2 molecule remains: $V_2H_6 + V_2H_6 \rightarrow V_4H_{10} + H_2$. The remaining H_2 has a substantial amount of kinetic energy with respect to the Si-bonded H and will start pressing on the surrounding matrix, which elevates n_∞

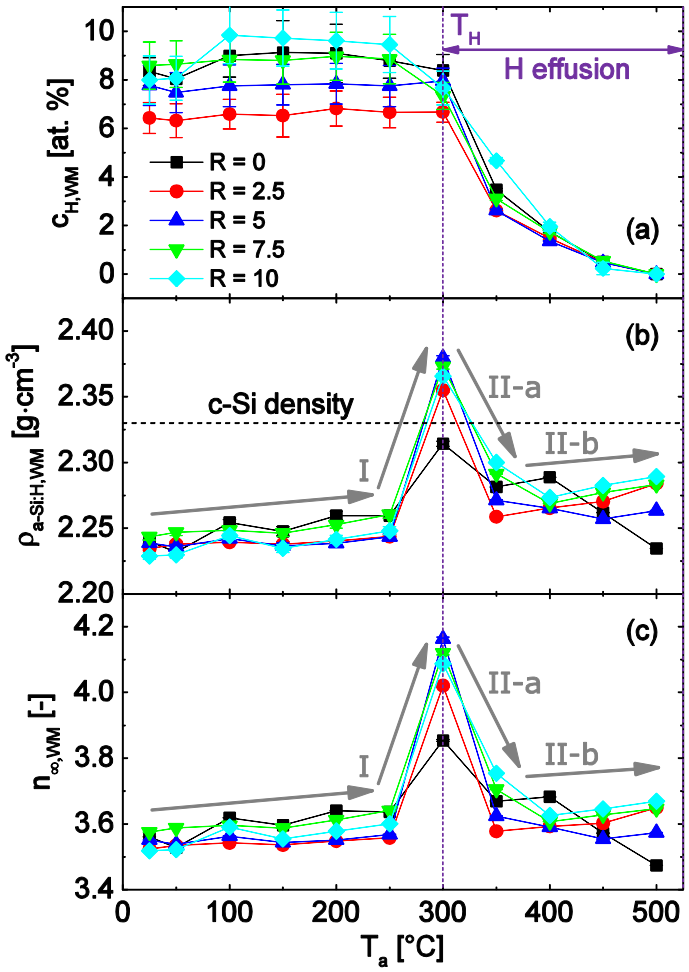

Fig. 3. Evolution of (a) the atomic hydrogen content, c_H, (b) the mass density, $\rho_{a\text{-}Si:H}$, and (c) the refractive index in the infrared, n_∞, during annealing for five dense a-Si:H films deposited at different R values. c_H, $\rho_{a\text{-}Si:H}$, and n_∞ are all calculated using the integrated absorption strength of the Si-H wagging modes (WM). Note that the error bars in (a) and (c) are fitting errors which are obtained when using a data fitting routine described elsewhere [80]. The error bars in (b) are obtained through an error propagation analysis using the fitting errors of the refractive index and the atomic hydrogen content in combination with the Clausius-Mosotti equation.

and consequently the calculated value of $\rho_{a\text{-}Si:H,WM}$ as well. When increasing the temperature further ($T_a > 300$ °C), the H effusion starts, as shown in Fig. 3a, which means that the material can relax so that n_∞ and thus also $\rho_{a\text{-}Si:H,WM}$ decrease again. Interestingly, such a relaxation directly linked to a c_H decrease has been previously explained as an intrinsic stress reduction [81]. Note that the $\rho_{a\text{-}Si:H,WM}$ peak value is higher for the $R > 0$ material when compared to the R = 0 material, implying that the earlier suggested reduced amount of vacancy migration in higher R materials yields a larger H_2-induced pressure build-up in open volume deficiencies. Note that the abrupt changes in $\rho_{a\text{-}Si:H,WM}$ can be more easily explained in the DNHV than they can in the CRN, in which voids are typically isolated. Additionally, there is an increase of 5% ± 1% in $\rho_{a\text{-}Si:H,WM}$ when increasing T_a from 250 °C to 300 °C, while only a gradual, small 2.4% ± 1.6% average decrease in the film thickness was observed for $T_a \leq 500$ °C, meaning that the

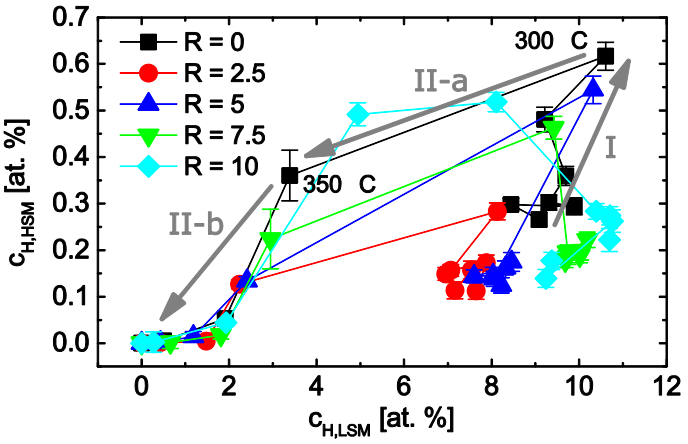

Fig. 4. Evolution of c_H corresponding to the Si-H low stretching modes (LSM) and high stretching modes (HSM) during annealing for five dense a-Si:H films deposited at different R values. Note that the error bars are fitting errors which are obtained when using a data fitting routine described elsewhere [80].

shrinkage of the film during annealing cannot explain the sharp increase in the density at T_a = 300 °C. It should be mentioned here that this increase is not due to an increase of the mass of the film or a sudden reduction of its volume, but is caused by the sudden increase in n_∞, since the density is calculated from the FTIR measurement data. Note that the thickness was determined by means of reflectance/transmittance measurements using a commercial system (supplied by W. Theiss Hard- and Software in combination with the SCOUT software) in the 375-1060 nm range. This means that several interference fringes were present in all measurements to enable an accurate determination of the thickness via standard thin-film optical models which use Fresnel amplitude coefficients to account for the interference between multiple reflections of the air/film/glass/air layer stack [34,82]. Furthermore, no significant changes in the phonon modes as determined by Raman spectroscopy were detected for $T_a \leq$ 500 °C, which otherwise might have been able to explain the $\rho_{a\text{-Si:H,WM}}$ peak at T_a = 300 °C in a CRN view.

When further analyzing the FTIR results, the local environment of the various Si-H bonds involved in the H effusion can be identified by an analysis of the SM. Particularly interesting are the two types of hydrogen effusion that can be clearly distinguished when considering the annealing-induced changes in the atomic hydrogen content in the LSM and HSM, $c_{H,LSM}$ and $c_{H,HSM}$, as depicted in Fig. 4. Process I is predominantly characterized by an increase in $c_{H,HSM}$, which can be explained as an increase in the number of Si-H bonds on the surface of large open volume deficiencies due to the clustering of small vacancies during annealing, which we concluded from the DB-PAS data shown in Fig. 2a. Note that we assume that the vast majority of small open volume deficiencies is fully hydrogenated in the as-deposited state, since only a very limited amount of small open volume deficiencies contains dangling bonds. The migrating hydrogen in the film can come from either Si-H bonds that were first contributing to the LSM, *i.e.* Si-H bonds at the surface of small open volume deficiencies such as divacancies, or it can be formed from non-silicon bonded hydrogen which can be present in the film in the as-deposited state. However, the latter process is highly unlikely since the H-H bond energy is significantly larger than the Si-H bond energy for a single bond in general (4.5 eV vs. ~3.1 eV [83]) and the various possible configurations of hydrogen in silicon (~1.65-3.60 eV [84]) in particular. Since the hydrogen content that is calculated from the wagging modes, as shown in Fig. 3a, does not show any large increase during the annealing experiment, but only a roughly continuous reduction when T_a > 300 °C, it can in fact be concluded that no large amounts of initially non-silicon bonded hydrogen are converted into Si-H bonds during annealing. What remains as a possible explanation for the increase in $c_{H,LSM}$ that appears at T_a = 300 °C is a change in the oscillator strength of the LSM, which could be induced by the accumulation of hydrogen in small open volume deficiencies. Since we used the same proportionality constants for the LSM and HSM throughout the annealing experiment for all samples and because it is impractical to determine the proportionality constants for each sample after each annealing step, it could be that this leads to an apparent increase of the hydrogen content at T_a = 300 °C when calculated from the stretching modes. Since the stretching modes are associated with Si-H oscillations perpendicular to the surface of open volume deficiencies while the wagging modes are linked to Si-H oscillations parallel to the surface of open volume deficiencies, it can be understood that the hydrogen content calculated from the wagging modes is unlikely to be affected by accumulating hydrogen in open volume deficiencies, while this can be the case for the hydrogen content calculated from the stretching modes. Furthermore, as was suggested based on the *S-W* diagram shown in Fig. 2c, process II-a can now be identified as hydrogen effusion from small open volume deficiencies, since it is predominantly $c_{H,LSM}$ that decreases and the LSM is known to be associated with DVs [55],[56]. Process II-b is characterized mostly by a decrease in $c_{H,HSM}$, which is linked to hydrogen effusion from large vacancy clusters and NVs. As an important consequence of this close connection between hydrogen effusion and vacancy agglomeration during annealing, we arrive at an alternative interpretation of hydrogen effusion measurements in terms of a two-stage process involving small vacancies and NVs, respectively. Hydrogen effusion measurements were previously typically explained by hydrogen effusion from interconnected voids (low temperature effusion) and isolated voids (high temperature effusion) [85].

D. Structural model describing the evolution of open volume deficiencies and Si-H bonds during annealing

For extra clarity the main evolution of vacancy clusters and hydrogen in a-Si:H during processes I, II-a, and II-b is summarized in Fig. 5, illustrated by representative examples of agglomeration reactions of vacancy clusters. The specific vacancies depicted here should be seen as general examples only, as slightly smaller and larger types of open volume deficiencies with fewer or more dangling bonds will likely be formed as well. During the clustering of DVs, which are predominantly present in the as-deposited state, small multivacancies like tetravacancies (V_4H_{10}) can be formed with an additional H_2 molecule present either in the surrounding CRN-like matrix or in the small vacancies themselves. Examples of these processes that are suggested to take place

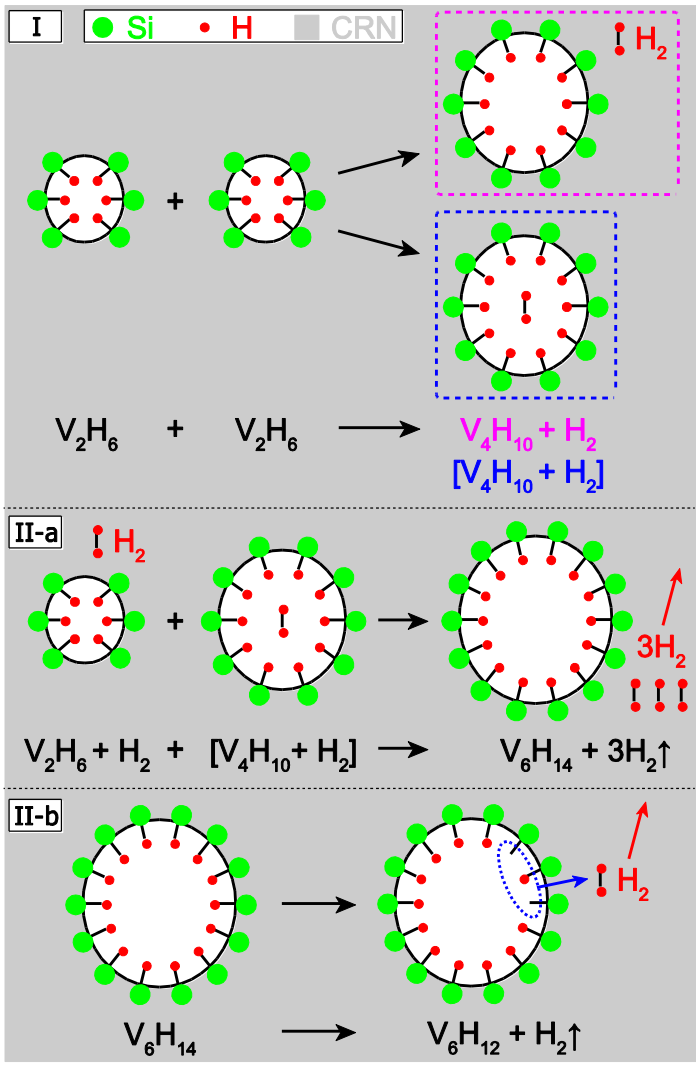

Fig. 5. Schematic drawing of the evolution of vacancy clusters and hydrogen during processes I, II-a and II-b: (I) vacancy agglomeration into larger vacancy clusters and trapping of hydrogen in the CRN environment surrounding the vacancy clusters and in the vacancy clusters themselves; (II-a) continued agglomeration into larger vacancy clusters and effusion of the previously trapped hydrogen; (II-b) hydrogen release from the surfaces of large vacancy clusters (and NVs) and subsequent hydrogen effusion.

during annealing are shown in Fig. 5. Generally, H_2 can reside in the a-Si:H material in two different environments. First, it can reside trapped inside an open volume deficiency and, secondly, it can be embedded in the CRN-like matrix which surrounds the open volume deficiencies. Although it is likely that both these configurations of H_2 result from process I, it is obvious from the DB-PAS and FTIR data that there is only an increase in $S/S_{c\text{-}Si}$ without large changes in the WM and SM for $T_a \leq 250$ °C. Therefore, we suspect a dominant formation of H_2 in the surrounding CRN matrix at $T_a \leq 250$ °C. Note that the trapping of H_2 is commonly known to depend on the annealing temperature [85]. Additionally, during process I it is highly likely that clustering of not fully hydrogen-passivated small vacancies, partially also with the involvement of non-silicon bonded hydrogen that is present in the as-deposited state, takes place in significant amounts as well, since the overall number of Si-H bonds is expected to remain roughly constant based on the FTIR data. Examples of such processes include $V_2H_6 + V_2H_4 \rightarrow V_4H_{10}$ and $V_2H_4 + V_3H_6 + H_2 \rightarrow V_5H_{12}$.

Only when $T_a = 300$ °C it is expected that the second possible outcome of process I, *i.e.* trapped H_2 in clustered small vacancies like tetravacancies, becomes more significant, which can explain the large peak in $\rho_{a\text{-}Si:H,WM}$ shown in Fig. 3b. Subsequently, the clustering of vacancies continues during process II-a while hydrogen effusion is starting to take place mostly from small vacancies. Note that this type of hydrogen effusion is derived from the dominant decrease in $c_{H,LSM}$ that occurs first when $T_a > 300$ °C. When T_a is increased even further, a dominant decrease in $c_{H,HSM}$ is observed, which is attributed to a release of hydrogen from the surface of large vacancies and NVs (process II-b). Finally, it should be noted that vacancy agglomeration can increase the H passivation degree of larger open volume deficiencies and hence reduce the metastable defect density. For example, the agglomeration of two divacancies of which one is not fully hydrogen-passivated, as can occur in process I, leads to a fully hydrogen-passivated tetravacancy: $V_2H_4 + V_2H_6 \rightarrow V_4H_{10}$. Such an improved hydrogen passivation degree could be the reason for the reduced LID that was recently observed for a-Si:H annealed at 350-400 °C prior to light soaking [86].

IV. Conclusions

The evolution of open volume deficiencies and hydrogen in a-Si:H films synthesized at various R values is monitored during annealing using a powerful combination of characterization tools based on DB-PAS and FTIR spectroscopy. The inferred reduced amount of open volume deficiency migration during annealing in more stable a-Si:H is an indication of an improved hydrogen passivation degree of open volume deficiencies and trapping of hydrogen in small multivacancy clusters during agglomeration of DVs. Additionally, an alternative interpretation of hydrogen effusion measurements is presented, pointing to a two-stage process involving small open volume deficiencies and nanosized voids, respectively, and schematic representations of the annealing-induced changes in the nanostructure are provided. These conclusions are relevant not only to the development of a-Si:H based solar cells, but could also be useful in understanding the nanostructure of other amorphous materials.

Acknowledgement

We acknowledge financial support for this research from ADEM, A green Deal in Energy Materials of the Ministry of Economic Affairs of The Netherlands (www.adem-innovationlab.nl), the STW Vidi project of A.H.M. Smets from Delft University of Technology.

References

[1] R.A. Street (ed.), "Technology and Applications of Amorphous Silicon," Springer-Verlag, Germany, 2000.

[2] A.H.M. Smets, K. Jäger, O. Isabella, R.A.C.M.M. van Swaaij, and M. Zeman, "Solar Energy – The Physics and Engineering of

Photovoltaic Conversion, Technologies and Systems," UIT Cambridge Ltd, United Kingdom, 2016.
[3] New Energy and Industrial Technology Development Organization (NEDO) and Kaneka Corporation, http://www.nedo.go.jp/english/news/AA5en_100109.html for "World's Highest Conversion Efficiency of 26.33% Achieved in a Crystalline Silicon Solar Cell—A World First in a Practical Cell Size," 2016.
[4] D.E. Polk, "Structural model for amorphous silicon and germanium," *J. Non-Cryst. Solids* vol. 5, pp. 365-376, 1971.
[5] D.K. Biegelsen and M. Stutzmann, "Hyperfine studies of dangling bonds in amorphous silicon," *Phys. Rev. B* vol. 33, no. 5, pp. 3006-3011, 1986.
[6] M. Stutzmann and D.K. Biegelsen, "Dangling or floating bonds in amorphous silicon," *Phys. Rev. Lett.* vol. 60, no. 16, p. 1682, 1988.
[7] H. Dersch, J. Stuke, and J. Beichler, "Light-induced dangling bonds in hydrogenated amorphous silicon," *Appl. Phys. Lett.* vol. 38, pp. 456-458, 1981.
[8] M. Stutzmann, W.B. Jackson, and C.C. Tsai, "Light-induced metastable defects in hydrogenated amorphous silicon," *Phys. Rev. B* vol. 32, no. 1, pp. 23-47, 1985.
[9] M. Stutzmann and D.K. Biegelsen, "Microscopic nature of coordination defects in amorphous silicon," *Phys. Rev. B* vol. 40, no. 14, pp. 9834-9840, 1989.
[10] Y. Bar-Yam and J.D. Joannopoulos, "Dangling bond in a-Si:H," *Phys. Rev. Lett.* vol. 56, no. 20, pp. 2203-2206, 1986.
[11] R.A. Street, J. Kakalios, and T.M. Hayes, "Thermal equilibration in doped amorphous silicon," *Phys. Rev. B* vol. 34, no. 4, pp. 3030-3033, 1986.
[12] Z.E. Smith and S. Wagner, "Band tails, entropy, and equilibrium defects in hydrogenated amorphous silicon," *Phys. Rev. Lett.* vol. 59, no. 6, pp. 688-691, 1987.
[13] H.M. Branz and E.A. Schiff, "Dangling-bond relaxation and deep-level measurements in hydrogenated amorphous silicon," *Phys. Rev. B* vol. 48, no. 12, pp. 8667-8671, 1993.
[14] S.T. Pantelides, "Defects in amorphous silicon: a new perspective," *Phys. Rev. Lett.* vol. 57, no. 23, pp. 2979-2982, 1986.
[15] J.H. Stathis and S.T. Pantelides, "Quantitative analysis of EPR and electron-nuclear double resonance spectra of *D* centers in amorphous silicon: dangling versus floating bonds," *Phys. Rev. B* vol. 37, no. 11, pp. 6579-6582, 1988.
[16] S.T. Pantelides, "Pantelides replies," *Phys. Rev. Lett.* vol. 60, no. 16, p. 1683, 1988.
[17] J.H. Stathis, "Analysis of the superhyperfine structure and the *g* tensor of defects in amorphous silicon," *Phys. Rev. B* vol. 40, no. 2, pp. 1232-1237, 1989.
[18] D.L. Staebler and C.R. Wronski, "Reversible conductivity changes in discharge-produced amorphous Si," *Appl. Phys. Lett.* vol. 31, pp. 292-294, 1977.
[19] D.L. Staebler and C.R. Wronski, "Optically induced conductivity changes in discharge-produced hydrogenated amorphous silicon," *J. Appl. Phys.* vol. 51, no. 6, pp. 3262-3268, 1980.
[20] S.T. Pantelides, "Defect dynamics and the Staebler-Wronski effect in hydrogenated amorphous silicon," *Phys. Rev. B* vol. 36, no. 6, pp. 3479-3482, 1987.
[21] W.B. Jackson, "Role of hydrogen complexes in the metastability of hydrogenated amorphous silicon," *Phys. Rev. B* vol. 41, no. 14, pp. 10257-10260, 1990.
[22] S.B. Zhang, W.B. Jackson, and D.J. Chadi, "Diatomic-hydrogen-complex dissociation: a microscopic model for metastable defect generation in Si," *Phys. Rev. Lett.* vol. 65, no. 20, pp. 2575-2578, 1990.
[23] P. Stradins and H. Fritzsche, "Photo-induced creation of metastable defects in a-Si:H at low temperatures and their effect on the photoconductivity," *Phil. Mag. B* vol. 69, no. 1, pp. 121-139, 1994.
[24] H.M. Branz, "Hydrogen collision model: quantitative description of metastability in amorphous silicon," *Phys. Rev. B* vol. 59, no. 8, pp. 5498-5512, 1999.
[25] C. Longeaud, D. Roy, and O. Saadane, "Role of interstitial hydrogen and voids in light-induced metastable defect formation in hydrogenated amorphous silicon: a model," *Phys. Rev. B* vol. 65, no. 085206, pp. 1-9, 2002.
[26] M.J. Powell, S.C. Deane, and R.B. Wehrspohn, "Microscopic mechanisms for creation and removal of metastable dangling bonds in hydrogenated amorphous silicon," *Phys. Rev. B* vol. 66, no. 155212, pp. 1-11, 2002.
[27] H. Fritzsche, "Development in understanding and controlling the Staebler-Wronski effect in a-Si:H," *Ann. Rev. Mater. Res.* vol. 31, pp. 47-79, 2001 (and references therein).
[28] T. Shimizu, "Staebler-Wronski effect in hydrogenated amorphous silicon and related alloy films," *Jpn. J. Appl. Phys.* vol. 43, no. 6A, pp. 3257-3268, 2004 (and references therein).
[29] J. Melskens, G. van Elzakker, Y. Li, and M. Zeman, "Analysis of hydrogenated amorphous silicon thin films and solar cells by means of Fourier Transform Photocurrent Spectroscopy," *Thin Solid Films* vol. 516, pp. 6877-6881, 2008.
[30] K.H. Kim, E.V. Johnson, A. Abramov, and P. Roca i Cabarrocas, "Light induced electrical and macroscopic changes in hydrogenated polymorphous silicon solar cells," *EPJ Photovolt.* vol. 3, no. 30301, pp. 1-14, 2012.
[31] S. Guha, J. Yang, and B. Yan, "High efficiency multi-junction thin film silicon cells incorporating nanocrystalline silicon," *Sol. Energy Mater. Sol. Cells* vol. 119, pp. 1-11, 2013 (and references therein).
[32] M. Stuckelberger, M. Despeisse, G. Bugnon, J.W. Schüttauf, F.-J. Haug, and C. Ballif, "Comparison of amorphous silicon absorber materials: light-induced degradation and solar cell efficiency," *J. Appl. Phys.* vol. 114, no. 154509, pp. 1-10, 2013.
[33] M. Boccard, M. Despeisse, J. Escarre, X. Niquille, G. Bugnon, S. Hänni, M. Bonnet-Eymard, F. Meillaud, and C. Ballif, "High-stable-efficiency tandem thin-film silicon solar cell with low-refractive-index silicon-oxide interlayer," *IEEE J. Photovolt.* vol. 4, no. 6, pp. 1368-1373, 2014.
[34] J. Melskens et al., "In situ manipulation of the sub gap states in hydrogenated amorphous silicon monitored by advanced application of Fourier transform photocurrent spectroscopy," *Sol. Energy Mater. Sol. Cells* vol. 129, pp. 70-81, 2014.
[35] S. Kirner, S. Neubert, C. Schultz, O. Gabriel, B. Stannowski, B. Rech, and R. Schlatmann, "Quadruple-junction solar cells and modules based on amorphous and microcrystalline silicon with high stable efficiencies," *Jpn. J. Appl. Phys.* vol. 54, no. 08KB03, pp. 1-8, 2015.
[36] A. Lambertz, F. Finger, R.E.I. Schropp, U. Rau, and V. Smirnov, "Preparation and measurement of highly efficient a-Si:H single junction solar cells and the advantages of μc-SiO_x:H n-layers," *Prog. Photovolt: Res. Appl.* vol. 23, no. 8, pp. 939-948, 2015.
[37] T. Matsui, A. Bidiville, K. Maejima, H. Sai, T. Koida, T. Suezaki, M. Matsumoto, K. Saito, I. Yoshida, and M. Kondo, "High-efficiency amorphous silicon solar cells: impact of deposition rate on metastability," *Appl. Phys. Lett.* vol. 106, no. 053901, pp. 1-5, 2015.
[38] H. Sai, T. Matsui, T. Koida, K. Matsubara, M. Kondo, S. Sugiyama, H. Katayama, Y. Takeuchi, I. Yoshida, "Triple-junction thin-film silicon solar cell fabricated on periodically textured substrate with a stabilized efficiency of 13.6%," *Appl. Phys. Lett.* vol. 106, no. 213902, pp. 1-4, 2015.
[39] J.-W. Schüttauf, B. Niesen, L. Löfgren, M. Bonnet-Eymard, M. Stuckelberger, S. Hänni, M. Boccard, G. Bugnon, M. Despeisse, F.-J. Haug, F. Meillaud, and C. Ballif, "Amorphous silicon-germanium for triple and quadruple junction thin-film silicon based solar cells, *Sol. Energy Mater. Sol. Cells* vol. 133, pp. 163-169, 2015.
[40] K.H. Kim, E.V. Johnson, and P. Roca i Cabarrocas, "Light-induced changes in silicon nanocrystal based solar cells:

modification of silicon-hydrogen bonding on silicon nanocrystal surface under illumination," *Jpn. J. Appl. Phys.* vol. 55, no. 072302, pp. 1-6, 2016.
[41] Y. Pan, F. Inam, M. Zhang, and D.A. Drabold, "Atomistic origin of Urbach tails in amorphous silicon," *Phys. Rev. Lett.* vol. 100, no. 206403, pp. 1-4, 2008.
[42] L.K. Wagner and J. C. Grossman, "Microscopic description of light induced defects in amorphous silicon solar cells," *Phys. Rev. Lett.* vol. 101, no. 265501, pp. 1-4, 2008.
[43] D.A. Drabold, Y. Li, B. Cai, and M. Zhang, "Urbach tails of amorphous silicon," *Phys. Rev. B* vol. 83, no. 045201, pp. 1-6, 2011.
[44] P.A. Khomyakov, W. Andreoni, N.D. Afify, and A. Curioni, "Large-scale simulations of a-Si:H: the origin of midgap states revisited," *Phys. Rev. Lett.* vol. 107, no. 255502, pp. 1-4, 2011.
[45] S. Zafar and E.A. Schiff, "Hydrogen and defects in amorphous silicon," *Phys. Rev. Lett.* vol. 66, no. 11, pp. 1493-1496, 1991.
[46] R. Biswas, Q. Li, Y. Yoon, and H.M. Branz, "Dangling-bond levels and structure relaxation in hydrogenated amorphous silicon," *Phys. Rev. B* vol. 56, no. 15, pp. 9197-9200, 1997.
[47] H.M. Branz, "Hydrogen diffusion and mobile hydrogen in amorphous silicon," *Phys. Rev. B* vol. 60, no. 11, pp. 7725-7727, 1999.
[48] A.H.M. Smets, C.R. Wronski, M. Zeman, and M.C.M. van de Sanden, "The Staebler-Wronski effect: new physical approaches and insights as a route to reveal its origin," *Mat. Res. Soc. Symp. Proc.* vol. 1245, no. A-14-02, pp. 1-6, 2010.
[49] J. Melskens, A.H.M. Smets, S.W.H. Eijt, H. Schut, E. Brück, and M. Zeman, "The nanostructural analysis of hydrogenated silicon films based on positron annihilation studies," *J. Non-Cryst. Solids* vol. 358, pp. 2015-2018, 2012.
[50] J. Melskens, A.H.M. Smets, M. Schouten, S.W.H. Eijt, H. Schut and M. Zeman, "New insights in the nanostructure and defect states of hydrogenated amorphous silicon obtained by annealing," *IEEE J. Photovolt.* vol. 3, no. 1, pp. 65-71, 2013.
[51] C.R. Wronski and X. Niu, "The limited relevance of SWE dangling bonds to degradation in high-quality a-Si:H solar cells," *IEEE J. Photovolt.* vol. 4, no. 3, pp. 778-784, 2014.
[52] M. Fehr et al., "Electrical detection of electron-spin-echo envelope modulations in thin-film silicon solar cells," *Phys. Rev. B* vol. 84, no. 245203, pp.1-5, 2011.
[53] M. Fehr, A. Schnegg, B. Rech, O. Astakhov, F. Finger, R. Bittl, C. Teutloff, and K. Lips, "Metastable defect formation at microvoids identified as a source of light-induced degradation in a-Si:H," *Phys. Rev. Lett.* vol. 112, no. 066403, pp. 1-5, 2014.
[54] J. Melskens, A. Schnegg, A. Baldansuren, K. Lips, M.P. Plokker, S.W.H. Eijt, H. Schut, M. Fischer, M. Zeman, and A.H.M. Smets, "Structural and electrical properties of metastable defects in hydrogenated amorphous silicon," *Phys. Rev. B* vol. 91, no. 245207, pp. 1-6, 2015.
[55] A.H.M. Smets, W.M.M. Kessels, and M.C.M. van de Sanden, "Vacancies and voids in hydrogenated amorphous silicon," *Appl. Phys. Lett.* vol. 82, no. 10, pp. 1547-1549, 2003.
[56] A.H.M. Smets and M.C.M. van de Sanden, "Relation of the Si-H stretching frequency to the nanostructural Si-H bulk environment," *Phys. Rev. B* vol. 76, no. 073202, pp. 1-4, 2007.
[57] M. Fischer, H. Tan, J. Melskens, R. Vasudevan, M. Zeman, and A.H.M. Smets, "High pressure processing of hydrogenated amorphous silicon solar cells: relation between nanostructure and high open-circuit voltage," *Appl. Phys. Lett.* vol. 106, no. 043905, pp. 1-5, 2015.
[58] H. Tan, E. Moulin, F.T. Si, J.-W. Schüttauf, M. Stuckelberger, O. Isabella, F.-J. Haug, C. Ballif, M. Zeman, and A.H.M. Smets, "Highly transparent modulated surfaces textured front electrodes for high-efficiency multijunction thin-film silicon solar cells," *Prog. Photovolt: Res. Appl.* vol. 23, no. 8, pp. 949-963, 2015.
[59] F.T. Si, D.Y. Kim, R. Santbergen, H. Tan, R.A.C.M.M. van Swaaij, A.H.M. Smets, O. Isabella, and M. Zeman, "Quadruple-junction thin-film silicon-based solar cells with high open-circuit voltage," *Appl. Phys. Lett.* vol. 105, no. 063902, pp. 1-5, 2014.
[60] L. Yang and L.-F. Chen, "The effect of H_2 dilution on the stability of a-Si:H based solar cells," *Mat. Res. Soc. Symp. Proc.* vol. 336, pp. 669-674, 1994.
[61] J. Yang, X. Xu, and S. Guha, "Stability studies of hydrogenated amorphous silicon alloy solar cells prepared with hydrogen dilution," *Mat. Res. Soc. Symp. Proc.* vol. 336, pp. 687-692, 1994.
[62] S. Guha, K.L. Narasimhan, and S.M. Pietruszko, "On light-induced effect in amorphous hydrogenated silicon," *J. Appl. Phys.* vol. 52, no. 2, pp. 859-860, 1981.
[63] S. Okamoto, Y. Hishikawa, and S. Tsuda, "New interpretation of the effect of hydrogen dilution of silane on glow-discharged hydrogenated amorphous silicon for stable solar cells," *Jpn. J. Appl. Phys.* vol 35, part 1, no. 1A, pp. 26-33, 1996.
[64] J. Melskens, M. Schouten, A. Mannheim, A.S. Vullers, Y. Mohammadian, S.W.H. Eijt, H. Schut, T. Matsui, M. Zeman, and A.H.M. Smets, "The nature and the kinetics of light-induced defect creation in hydrogenated amorphous silicon films and solar cells," *IEEE J. Photovolt.* vol. 4, no. 6, pp. 1331-1336, 2014.
[65] G. van Elzakker, V. Nádaždy, F.D. Tichelaar, J.W. Metselaar, and M. Zeman, "Analysis of structure and defects in thin silicon films deposited from hydrogen diluted silane," *Thin Solid Films* vol. 511-512, pp. 252-257, 2006.
[66] R.W. Collins, A.S. Ferlauto, G.M. Ferreira, C. Chen, J. Koh, R.J. Koval, Y. Lee, J.M. Pearce, and C.R. Wronski, "Evolution of microstructure and phase in amorphous, protocrystalline, and microcrystalline silicon studied by real time spectroscopic ellipsometry," *Sol. Energy Mater. Sol. Cells* vol. 78, pp. 143-180, 2003.
[67] A.H.M. Smets, W.M.M. Kessels, and M.C.M. van de Sanden, "Temperature dependence of the surface roughness evolution during hydrogenated amorphous silicon growth," *Appl. Phys. Lett.* vol. 82, no. 6, pp. 865-867, 2003.
[68] W.M.M. Kessels, J.P.M. Hoefnagels, E. Langereis, and M.C.M. van de Sanden, "Substrate temperature dependence of the roughness evolution of HWCVD a-Si:H studied by real-time spectroscopic ellipsometry," *Thin Solid* Films vol. 501, no. 1-2, pp. 88-91, 2006.
[69] A. van Veen, H. Schut, J. de Vries, R.A. Hakvoort, and M.R. IJpma, "Analysis of positron profiling data by means of VEPFIT", *AIP Conf. Proc.* vol. 218, pp. 171-196, 1991.
[70] A. van Veen, H. Schut, and P.E. Mijnarends, "Depth-profiling of subsurface regions, interfaces and thin films" in *Positron Beams and Their Applications*, edited by P.G. Coleman, ch. 6, pp. 191-225, World Scientific, Singapore, 2000.
[71] H. Schut, "A variable energy positron beam facility with applications in materials science," Ph.D. dissertation, Faculty of Applied Sciences, Delft University of Technology, Delft, the Netherlands, 1990.
[72] R.A. Hakvoort, "Applications of positron depth profiling," Ph.D. dissertation, Faculty of Applied Sciences, Delft, University of Technology, Delft, the Netherlands, 1993.
[73] P.J. Schultz and K.G. Lynn, "Interaction of positron beams with surfaces, thin films, and interfaces," *Rev. Mod. Phys.* vol. 60, no. 3, pp. 701-781, 1988.
[74] D.E. Carlson, "Hydrogenated microvoids and light-induced degradation of amorphous silicon solar cells," *Appl. Phys. A* vol. 41, pp. 305-309, 1986.
[75] D.E. Carlson, "Hydrogen motion and the Staebler-Wronski effect in amorphous silicon" in *Disordered Semiconductors*, edited by M.A. Kastner, G.A. Thomas, and S.R. Ovshinsky, pp. 613-620, Plenum Press, New York, USA and London, United Kingdom, 1987.
[76] S. Acco, D.L. Williamson, W.G.J.H.M. van Sark, W.C. Sinke, W.F. van der Weg, A. Polman, and S. Roorda, "Nanoclustering of hydrogen in ion-implanted and plasma-grown amorphous silicon," *Phys. Rev. B* vol. 58, no. 19, pp. 12853-12864, 1998.

[77] J.A. Reimer, R.W. Vaughan, and J.C. Knights, "Proton NMR studies of annealed plasma-deposited amorphous Si:H films," *Solid State Commun.* vol. 37, no. 2, pp. 161-164, 1981.

[78] S. Yamasaki, S. Kuroda, K. Tanaka, and S. Hayashi, "Hyperfine interaction between hydrogens and dangling bonds in a-Si:H studies by ENDOR," *Solid State Commun.* vol. 50, no. 1, pp. 9-11, 1984.

[79] Z. Remeš, M. Vaněček, P. Torres, U. Kroll, A.H. Mahan, and R.S. Crandall, "Optical determination of the mass density of amorphous and microcrystalline silicon layers with different hydrogen contents," *J. Non-Cryst. Solids* vol. 227-230, pp. 876-879, 1998.

[80] R.J. Severens, G.J.H. Brussaard, M.C.M. van de Sanden, and D.C. Schram, "Characterization of plasma beam deposited amorphous hydrogenated silicon," *Appl. Phys. Lett.* vol. 67, pp. 491-493, 1995.

[81] E. Spanakis, E. Stratakis, P. Tzanetakis, and Q. Wang, "Elastic properties, intrinsic and photo-induced stress in hydrogenated amorphous silicon thin films with different hydrogen content," *J. Appl. Phys.* vol. 89, no. 8, pp. 4294-4300, 2001.

[82] M. Born and E. Wolf, "Principles of optics," 7th ed., Cambridge University Press, pp. 54-74, 1999.

[83] L. Pauling, "The nature of the chemical bond and the structure of molecules and crystals: an introduction to modern structural chemistry," 3rd ed., Cornell University Press, New York, NY, United States of America, p. 85, 1960.

[84] C.G. van de Walle, "Hydrogen in semiconductors II, Semiconductors and semimetals volume 61," N.H. Nickel (ed.), Academic Press, San Diego, CA, United States of America, p. 246, 1999.

[85] W. Beyer, "Diffusion and evolution of hydrogen in hydrogenated amorphous and microcrystalline silicon," *Sol. Energy Mater. Sol. Cells* vol. 78, pp. 235-267, 2003.

[86] D.C. Bobela, H.M. Branz, and P. Stradins, "Anneal treatment to reduce the creation rate of light-induced metastable defects in device-quality hydrogenated amorphous silicon," *Appl. Phys. Lett.* vol. 98, no. 201908, pp. 1-3, 2011.